VNU Journal of Science: Mathematics - Physics

Journal homepage: https://js.vnu.edu.vn/MaP

Original Article

Study of Crystallization Kinetics of $(Fe_{50}Ni_{50})_{73.5}Si_{13.5}B_9Nb_3Cu_1$ Ribbons Prepared by Rapid Cooling Technique

Nguyen Quang Hoa, Do Thi Kim Anh, Nguyen Duy Thien, Hoang Van Huy, Tran Vinh Thang, Nguyen Ngoc Dinh, Tran Thi Ngoc Anh, Luong Thi Minh Thuy, Vuong Van Hiep*

VNU University of Science, 334 Nguyen Trai, Thanh Xuan, Hanoi, Vietnam

Received 03 March 2023
Revised 13 March 2023; Accepted 13 March 2023

Abstract: Amorphous alloy ribbons of $(Fe_{50}Ni_{50})_{73.5}Si_{13.5}B_9Nb_3Cu_1$ were fabricated by rapid cooling technique on single copper wheel. After fabrication, the crystalline structure of the ribbons were examined by X-ray diffraction method. The results show that the samples possess a complete amorphous state. The crystallization process was studied by using a differential thermal analyzer (DSC). The DSC analysis show that there are two exothermic peaks corresponding to two crystalline phases appeared in the alloy ribbons. By changing the heating rate (i.e. 5, 10, 15, 20 and 25 ^oC/min) and by using the Kissinger method, The activation energy of crystallization of the crystalline phases determined for one phase was found to be E_1 = 350 kJ/mol and for other one, E_2 = 375 kJ/mol. Based on these results, we have chosen the appropriate annealing mode for the alloy ribbons. After annealing, the alloy ribbons were achieved nanocrystalline states of FeNi and α-Fe nano-particles with the grain size ranging from 5 to 15 nm and the fraction of crystallization between the crystalline and amorphous phases of 46, 67, 85 and 96 % respectively for the annealing regimes at 500 ^oC for 20, 30, 50 and 60 minutes.

Keywords: Amorphous, alloy, ribbons, α-Fe, crystallization, activation energy, DSC.

1. Introduction

Amorphous alloys of a composition of (Fe,Ni,Co)-Si-B-Nb-Cu with adjunct portion of nanocrystals are ultralsoft magnetic materials having very small coercive force H_c, high permeability μ, and are

* Corresponding author.
E-mail address: vuonghiepcms@gmail.com

https//doi.org/10.25073/2588-1124/vnumap.4837

widely used in industry. The alloy ribbons in amorphous state are heat treated to form crystalline phases with nanometer-size particles. These nano-sized crystals strongly reduce the effective magnetic anisotropy of the alloys. The appropriate ratio of the amorphous phase to the crystalline phase will result in a compensation between the negative magnetostriction of the crystalline phase and the residual positive magnetostriction of the amorphous phase. The appropriate grain size and crystalline phase ratio will provide to the alloy with best soft magnetic properties [1-7]. According to the previous researches of Herger [8, 9], the nanocrystalline alloys on amorphous substrates possess multiphase structures, including both the crystalline and the amorphous phases. The crystalline phase usually consists of Fe(Si) particles with size D = 10÷20 nm. This size is smaller than the exchange interaction length ($D << L_{ex}$), so the related magnetic anisotropy is replaced by the effective magnetic anisotropy $\langle K \rangle \sim D^6$ [10]. The soft magnetic properties of the nanocrystalline alloys depend heavily on the elemental composition, phase composition and fabrication technology. In this work, we present the fabrication and investigation of crystallization kinetics of $(Fe_{50}Ni_{50})_{73.5}Si_{13.5}B_9Nb_3Cu_1$ alloy ribbons under different heat treatment conditions.

2. Experiment

Amorphous alloy ribbons of $(Fe_{50}Ni_{50})_{73.5}Si_{13.5}B_9Nb_3Cu_1$ composition with appropriate crystalline phase are fabricated by rapid cooling on single rotating copper wheel at a cooling speed not less than 10^6 $^oC/s$. The resulting ribbons have a thickness of about 20 μm and a width of 10 mm. The possible phases of ribbons before and after annealing were investigated by X-ray diffraction using Cu-Kα radiation with wavelength λ = 1.54056 Å. The analysis of phase transition temperatures and the crystallization activation energy were performed on a differential thermal analyzer Thermoplus EV02 (DSC 8231). Alloy ribbons were annealed at 500 ^oC for different times (i.e. at from 10 to 60 minutes) on an XD 1600MT annealing furnace in a protective Ar atmosphere. We compared the DSC result from the alloy sample without annealing with the one from the annealed alloy sample, then we determined the crystallization activation energy and the corresponding fraction of the crystalline phase.

3. Rerults and Discussion

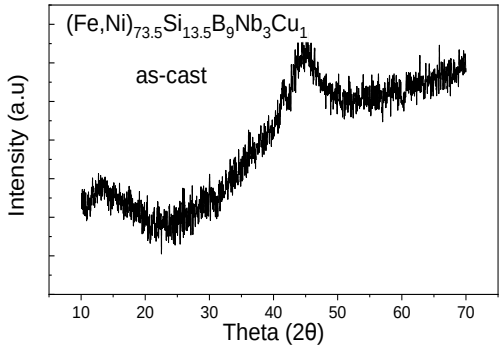

Figure 1. X-ray diffraction patterns of as-cast $(Fe_{50}Ni_{50})_{73.5}Si_{13.5}B_9Nb_3Cu_1$ ribbon.

Fig. 1 presents the X-ray diffraction patterns of as-cast $(Fe_{50}Ni_{50})_{73.5}Si_{13.5}B_9Nb_3Cu_1$ ribbon. It shows that the patterns exhibit only one broad peak around $2\theta \sim 45^o$, therefore the ribbon sample exhibits almost amorphous structure. The results of DSC analysis on amorphous ribbon performed with heating

rates from 5 °C/min to 25 °C/min in the temperature range from room temperature to 650 °C are presented in Fig. 2. From this figure, it is clear that there are two exothermic peaks of crystallization starting from about 500 °C to 580 °C. The first peak and the second peak appeared, respectively corresponding to with the crystallization of FeNi phase and α-Fe phase, which is consistent with the results of the previous work [5, 6].

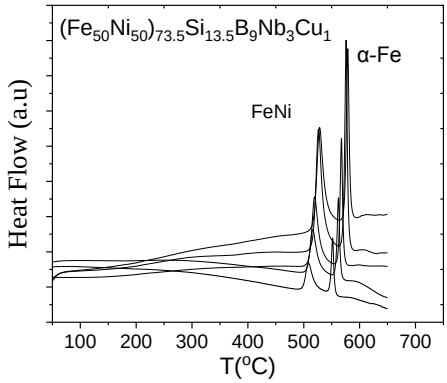

Figure 2. DSC curves with different heating rates of ribbons $(Fe_{50}Ni_{50})_{73.5}Si_{13.5}B_9Nb_3Cu_1$.

From the DSC curves of the ribbon with different heating rates, the crystallization activation energy can be calculated based on the Kissinger formula [10]:

$$\ln\left(\frac{\beta}{T_p^2}\right) = -\frac{E}{R}.\frac{1}{T_p} + const\ . \quad (1)$$

where β is the heating rate, T_p temperature at exothermal peak, k_B the Boltzmann constant and E the activation energy of crystallization.

Fig. 3 shows that the Kissinger curve (Eq. 1) is almost straight. From the slopes of the straight line, one can calculate the crystallization activation energy, and it was found to be E_1 = 350 kJ/mol for FeNi phase, and E_2 = 375 kJ/mol for α-Fe phase. These values are close to 413 and 418 kJ/mol for the Finemet [12].

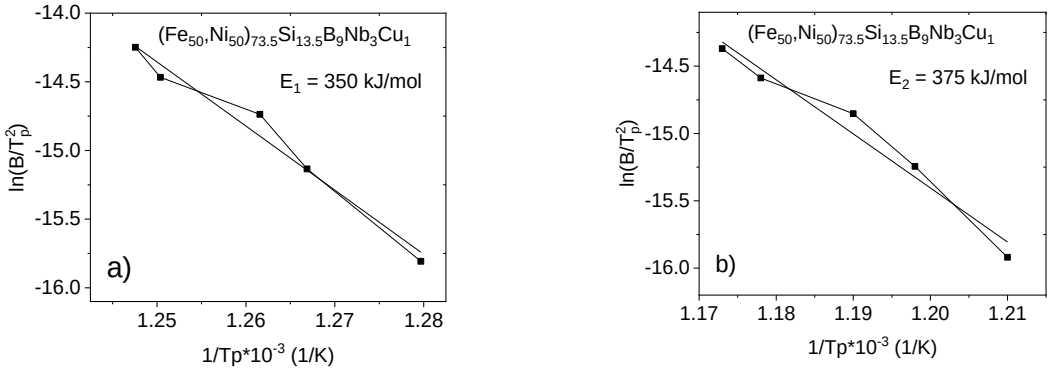

Figure 3. Kissinger plots for determination of crystallization activation energy of FeNi (a) and α-Fe (b) phase.

Fig. 4 shows the results of DSC measurement of the as-cast and annealed ribbons (500 °C for 20 minutes) $(Fe_{50}Ni_{50})_{73.5}Si_{13.5}B_9Nb_3Cu_1$. After annealing, the ribbons appeared partially crystallized, then when measured by DSC, the area containing the exothermic peak of crystallization is smaller than that of the as-cast sample.

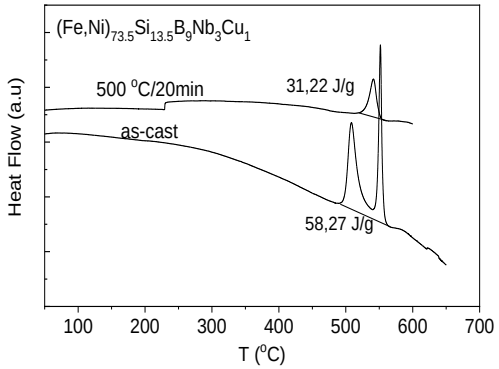

Figure 4. DSC curves of as-cast and annealed ribbons $(Fe_{50}Ni_{50})_{73.5}Si_{13.5}B_9Nb_3Cu_1$for estimation of thecrystallization volume fraction.

The fraction of crystallinity of the amorphous alloys that are heat treated at 500 °C for different time periods is determined by the formula [13]:

$$\chi_f = \frac{\Delta H_a - \Delta H_t}{\Delta H_a} \quad (2)$$

where ΔH_a and ΔH_t are the crystallization enthalpies of the as-cast sample and of the sample annealed for the time t, respectively. The calcutation results are presented in Table 1.

Fig. 5 shows the X-ray diffraction patterns of $(Fe_{50}Ni_{50})_{73.5}Si_{13.5}B_9Nb_3Cu_1$ ribbon measured after annealing at 500 °C for 20 to 60 minutes. One can see that the intensity of the diffraction peak at the angle of $2\theta \approx 45^o$ corresponding to the FeNi and α-Fe crystalline phases increases with the increase of the annealing time, that is consistent with the increase in crystallization rate presented in Table 1.

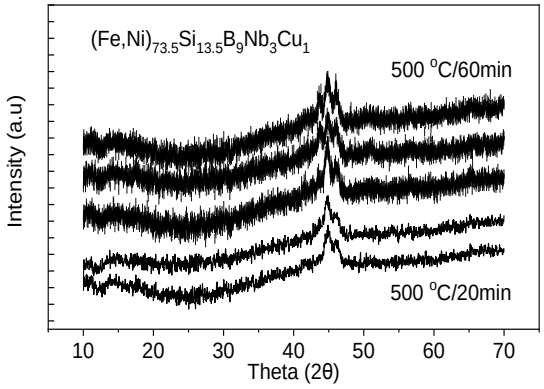

Figure 5. X-ray diffraction patterns of annealed ribbons $(Fe_{50}Ni_{50})_{73.5}Si_{13.5}B_9Nb_3Cu_1$($T_a$= 500 °C and 20–60 min).

Also, from Fig. 5, one can calculate the average size of the crystal grains to be in the range from 5 to 15 nm (Table 1) by using the Sherrer formula [14]:

$$D = \frac{0.9\lambda}{\beta.\cos(\theta_B)} \quad (3)$$

where D is the mean size of the crystalline particle, λ the X-ray wavelength, β the line broadening, i.e.the half width at the maximum of intensity peak, θ the Bragg angle.

Table 1. The crystallinity fraction and average grain size of the alloys $(Fe_{50}Ni_{50})_{73.5}Si_{13.5}B_9Nb_3Cu_1$ annealed at 500 ºC for 20-60 minutes

Time (minutes)	20	30	40	50	60
Crystallization fraction (%)	46	67	-	85	96
D (nm)	5	8	10	12	15

4. Conclusion

Research on the crystallization process of the amorphous alloy ribbon $(Fe_{50}Ni_{50})_{73.5}Si_{13.5}B_9Nb_3Cu_1$ fabricated by rapid cooling method, followed by annealing at 500 ºC for different periods of time shows that the heat treatment time of about 50 minutes is enough to obtain FeNi and α-Fe crystalline phases of about 85% with the grain size of ~ 12 nm and the crystallization activation energy of E_1 = 350, E_2 = 375 kJ/mol, respectively. The obtained results contributed to the elucidation of the formation and growth process of crystal grains. Therefore, it helps to apply the technological regime in order to manufacture the alloys with necessary properties.

Acknowledgments

This work was supported by the research project from VNU University of Science (TN), the research project code: TN.22.04

References

[1] Y. Yoshizawa, S. Oguwa, K. Yamaguchi, New Febased Soft Magnetic Alloys Composed of Ultrafine Grain Structure, J. Appl. Phys., Vol. 64 ,1988, pp. 6044, https://doi.org/10.1063/1.342149.

[2] Dipti Ranjan Sahu, Functional Materials, IntechOpen, London, 2019.

[3] A. V. Nosenko, V. V. Kyrylchuk, M. P. Semenko, M. Nowicki, A. Marusenkov, T. M. Mika, O. M. Semyrga, G. M. Zelinska, V. K. Nosenko, Soft Magnetic Cobalt Based Amorphous Alloys with Low Saturation Induction, J. Magn. Magn. Mater., Vol. 515, 2020, pp. 167328, https://doi.org/10.1016/j.jmmm.2020.167328.

[4] D. T. H. Gam, N. H. Hai, L. V. Vu, N. H. Luong, N. Chau, Influence of Cooling Rate on the Properties of $Fe_{73.5}Si_{13.5}B_9Nb_3Au_1$ ribbons, VNU Journal of Science, Mathematics – Physics, Vol. 24, 2008, pp. 189.

[5] N. Chau, N. Q. Hoa, N. D. The, L. V. Vu, The effect of Zn, Ag and Au Substitution for Cu in Finemet on the Crystallization and Magnetic Properties, J. Magn. Magn. Mater., Vol. 303, 2006, pp. e415, https://doi.org/10.1016/j.jmmm.2006.01.057.

[6] N. Chau, N. Q. Hoa, N. D. The, P. Q. Niem, Ultrasoft Magnetic Properties in Nanocrystalline Alloy Finemet with Au Substituted for Cu, J. Magn. Magn. Mater., Vol. 304, 2006, pp. e179, https://doi.org/10.1016/j.jmmm.2006.01.225.

[7] M. Zhu, C. Zhang, T. Xu, L. Yao, Y. Liu, M. Cai, Z. Jian, Glass Formation, Magnetic Properties, and Electrical Resistivity of the Multi-component FeNbBCuNiCo Amorphous Alloys, Int. J. Mater. Res., Vol. 112, 2021, pp. 2, https://doi.org/10.1515/ijmr-2020-1104.

[8] N. Chau, N. X. Chien, N. Q. Hoa, P. Q. Niem, N. H. Luong, N. D. Tho, V. V. Hiep, Investigation of Nanocomposite Materials with Ultrasoft and High Performance Hard Magnetic Properties, J.Magn. Magn. Mater., Vol. 282, 2004, pp. 174, https://doi.org/10.1016/j.jmmm.2004.04.041.

[9] G. Herzer, Grain Structure and Magnetism of Nanocrystalline Ferromagnets, Ieee Trans. Magn., Vol. 25, 1989, pp. 3327, https://doi.org/10.1109/20.42292.

[10] G. Herzer, Grain Size Dependence of Coercivity and Permeability in Nanocrystalline Ferromagnets, Ieee Trans, Magn., Vol. 26, No. 5, 1990, pp. 1397, https://doi.org/10.1109/20.104389.

[11] H. Kissinger, Reaction Kinetics in Differential Thermal Analysis, Anal. Chem., Vol. 29, 1957, pp. 1702, https://doi.org/10.1021/ac60131a045.

[12] G. Herzer, Soft Magnetic Nanocrystalline Materials, Scr. Metall. Mater., Vol. 33, No. 10-11, 1995, pp. 1741, https://doi.org/10.1016/0956-716X(95)00397-E.

[13] M. S. Leu, T. S. Chin, Quantitative Crystallization and Nano-Grain Size Distribution Studies of a Fecunbsib Nanocrystalline Alloy, MRS Symp. Proc., Vol. 577, 1999, pp. 557.

[14] B. E. Warren, X-ray Diffraction, Dover Publications, New York, 1990.